Mixed Ruthenium–Rhodium Trinuclear Complex $[Ru_2Rh(\mu_3\text{-}O)(\mu\text{-}CH_3COO)_6(L)_3]^+$ (L = H_2O or Pyridine)

Yoichi Sasaki,* Ayako Tokiwa, and Tasuku Ito*

Contribution from the Department of Chemistry, Faculty of Science, Tohoku University, Aoba, Aramaki, Sendai 980, Japan. *Received February 23, 1987*

Abstract: The preparation and purification method of a new ruthenium(III)–rhodium(III) cluster, $[Ru_2Rh(\mu_3\text{-}O)(\mu\text{-}CH_3COO)_6(L)_3]^+$ (L = H_2O or pyridine (py)), are described. The mixed-metal structure was confirmed by the ^1H and ^{13}C NMR spectra (splitting of all the signals to a 1:2 intensity ratio) and the metal 3d electron signal intensities of the X-ray photoelectron spectra. The mixed-metal aqua and pyridine complexes exhibit an intense visible absorption peak at 576 nm (ϵ 2000 M^{-1} cm^{-1}) and 590 (3980), respectively. Three reversible one-electron-redox waves are observed at +1.68, +0.79, and −0.78 V vs the Ag/Ag^+ electrode for the pyridine complex in CH_3CN and are assigned to $[Ru_2Rh]^{3+/2+}$, $[Ru_2Rh]^{2+/+}$, and $[Ru_2Rh]^{+/0}$, respectively. The ^1H NMR spectrum of the aqua complex in CD_3OD changes slowly as the substitution of CD_3OD for the aqua ligands takes place, first-order rate constants being 6.0×10^{-5} (per Ru) and 1.2×10^{-4} s^{-1} at the ruthenium and the rhodium centers, respectively, at 21 °C.

Preparation of new mixed-metal clusters is important for understanding metal–metal interactions within a cluster unit as well as developing new types of reactivities including redox and site-selective ligand substitution reactions.[1] Mixed-metal compounds are known for a number of carbonyl and related organometallic clusters,[2] but only a few are known for non-carbonyl-type clusters,[3-15] in which metal ions are less perturbed electronically by ligands. We have initiated the study of mixed-metal non-carbonyl clusters and recently reported the preparation of mixed molybdenum–tungsten clusters (Figure 1a), $[Mo_2W(\mu_3\text{-}O)_2(\mu\text{-}CH_3COO)_6(H_2O)_3]^{2+}$ and $[MoW_2(\mu_3\text{-}O)_2(\mu\text{-}CH_3COO)_6(H_2O)_3]^{2+}$,[14] together with their various spectroscopic properties including metal NMR[16] and X-ray photoelectron spectra.[17] It has been suggested that the tungsten and the molybdenum ions in the mixed-metal clusters possess somewhat higher and lower oxidation states, respectively, than in the homometal clusters, $[M_3(\mu_3\text{-}O)_2(\mu\text{-}CH_3COO)_6(H_2O)_3]^{2+}$ (M = Mo or W[18]).[17]

It is preferable to prepare mixed-metal clusters whose structural parameters are similar to their homometal analogues, since for such mixed-metal clusters electronic structures and reactivities can be discussed without considering serious influence from steric factors. In the above example, all the homo- and heterometal clusters (Mo_3, Mo_2W, MoW_2, and W_3) have very similar structural characteristics to one another (i.e. metal–metal bond lengths (ca. 2.72 Å) and other bond lengths and angles are almost identical among the four cluster ions[14,19,20]). The clusters of this type, which have direct metal–metal bonding interactions,[18] are also known for niobium.[21]

Similar trinuclear complexes but with one μ_3-oxo ligand in the center of a metal triangle are known for a much wider range of metal ions (Figure 1b:[22,23] i.e., tervalent metal ions such as V,[24] Cr,[25] Mn,[26] Fe,[27] Co,[28] Ru,[29,30] Rh,[31,32] and Ir.[23] Thus this type of complex provides another system appropriate for the study of

(1) For example: Hidai, M.; Matsuzaka, H.; Koyasu, Y.; Uchida, Y. *J. Chem. Soc., Chem. Commun.* **1986**, 1451–1452.
(2) For recent examples: (a) Abad, J. A.; Delgado, E.; Garcia, M. E.; Grosse-Ophoff, M. J.; Hart, I. J.; Jeffery, J. C.; Simmons, M. S.; Stone, F. G. A. *J. Chem. Soc., Dalton trans.* **1987**, 41–50, and related papers. (b) Blohm, M. L.; Gladfelter, W. L. *Inorg. Chem.* **1987**, *26*, 459–463. (c) Do, Y.; Knobler, C. B.; Hawthorne, M. F. *J. Am. Chem. Soc.* **1987**, *109*, 1853–1854. (d) Nagaki, D. A.; Badding, J. V.; Stacy, A. M.; Dahl, L. F. *J. Am. Chem. Soc.* **1986**, *108*, 3825–3827. (e) Adams, R. D.; Babin, J. E.; Mahtab, R.; Wang, S. *Inorg. Chem.* **1986**, *25*, 1623–1631.
(3) Some mixed-metal sulfur clusters: (a) Carney, M. J.; Kovacs, J. A.; Zhang, Y.-P.; Papaefthymiou, G. C.; Spartalian, K.; Frankel, R. B.; Holm, R. H. *Inorg. Chem.* **1987**, *26*, 719–724. (b) Shibahara, T.; Akashi, H.; Kuroya, H. *J. Am. Chem. Soc.* **1986**, *108*, 1342–1343, and references therein.
(4) Weinland, R.; Gussmann, E. *Ber. Dtsch. Chem. Ges.* **1909**, *42*, 3881–3894.
(5) Matson, M. S.; Wentworth, R. A. D. *J. Am. Chem. Soc.* **1974**, *96*, 7837–7839.
(6) Garner, C. D.; Senior, R. G.; King, T. J. *J. Am. Chem. Soc.* **1976**, *98*, 3526–3529.
(7) Glowiak, T.; Kubiak, M.; Szymanska-Buzar, T.; Jezowska-Trzebiatowska, B. *Acta Crystallogr., Sect. B: Struct. Crystallogr. Cryst. Chem.* **1977**, *B33*, 3106–3109.
(8) Katovic, V.; McCarley, R. E. *J. Am. Chem. Soc.* **1978**, *100*, 5586–5587.
(9) Clegg, W.; Lam, O. M.; Straughan, B. P. *Angew. Chem., Int. Ed. Engl.* **1984**, *23*, 434–435.
(10) Chisholm, M. H.; Folting, K.; Huffman, J. C.; Kober, E. M. *Inorg. Chem.* **1985**, *24*, 241–245.
(11) Chisholm, M. H.; Folting, K.; Hepert, J. A.; Hoffman, D. M.; Huffman, J. C. *J. Am. Chem. Soc.* **1985**, *107*, 1234–1241.
(12) Straughan, B. P.; Lam, O. M. *Inorg. Chim. Acta* **1985**, *98*, 7–10.
(13) Bursten, B. E.; Cotton, F. A.; Cowley, A. H.; Hanson, B. E.; Lattman, M.; Stanley, G. G. *J. Am. Chem. Soc.* **1979**, *101*, 6244–6249.
(14) Wang, B.; Sasaki, Y.; Nagasawa, A.; Ito, T. *J. Am. Chem. Soc.* **1986**, *108*, 6059–6060.
(15) Straughan, B. P.; Lam, O. M.; Earnshaw, A. *J. Chem. Soc., Dalton Trans.* **1987**, 97–99.
(16) Nagasawa, A.; Sasaki, Y.; Wang, B.; Ikari, S.; Ito, T. *Chem. Lett.* **1987**, 1271–1274.
(17) Wang, B.; Sasaki, Y.; Ikari, S.; Kimura, K.; Ito, T. *Chem. Lett.*, in press.
(18) Cotton, F. A. *Polyhedron* **1986**, *5*, 3–14.
(19) Ardon, M.; Bino, A.; Cotton, F. A.; Kaftory, M.; Reisner, G. *Inorg. Chem.* **1982**, *21*, 1912–1917.
(20) Bino, A.; Hesse, K.-F.; Kuppers, H. *Acta Crystallogr., Sect. B: Struct. Crystallogr. Cryst. Chem.* **1980**, *B36*, 723–725.
(21) (a) Cotton, F. A.; Duraj, S. A.; Roth, W. J. *J. Am. Chem. Soc.* **1984**, *106*, 3527–3531. (b) Cotton, F. A.; Diebold, M. P.; Ilusar, R.; Roth, W. J. *J. Chem. Soc., Chem. Commun.* **1986**, 1276–1278, and references therein.
(22) (a) Catterick, J.; Thornton, P. *Adv. Inorg. Chem. Radiochem.* **1977**, *20*, 291–362. (b) Mehrotra, R. C.; Bohra, R. *Metal Carboxylates*; Academic: London, 1983.
(23) Uemura, S.; Spencer, A.; Wilkinson, G. *J. Chem. Soc., Dalton Trans.* **1973**, 2565–2571.
(24) (a) Glowiak, T.; Kubiak, M.; Jezowska-Trzebiatowska, B. *Bull. Acad. Pol. Sci., Ser. Sci. Chim.* **1977**, *25*, 359–371. (b) Cotton, F. A.; Extine, M. W.; Falvello, L. R.; Lewis, D. B.; Lewis, G. E.; Murillo, C. A.; Schwotzer, W.; Tomas, M.; Troup, J. M. *Inorg. Chem.* **1986**, *25*, 3503–3512.
(25) (a) Chang, S. C.; Jeffrey, G. A. *Acta Crystallogr., Sect. B: Struct. Crystallogr. Cryst. Chem.* **1970**, *B26*, 673–683. (b) Figgis, B. N.; Robertson, G. B. *Nature (London)* **1965**, *205*, 694–695. (c) Wrobleski, J. T.; Dziobkowski, C. T.; Brown, D. B. *Inorg. Chem.* **1981**, *20*, 684–686.
(26) Hessel, L. W.; Romers, C. *Recl. Trav. Chim. Pays-Bas* **1969**, *88*, 545–552.
(27) Anzenhofer, K.; DeBoer, J. J. *Recl. Trav. Chim. Pays-Bas* **1969**, *88*, 286–288.
(28) Sumner, C. E., Jr.; Steinmetz, G. R. *J. Am. Chem. Soc.* **1985**, *107*, 6124–6126.
(29) Spencer, A.; Wilkinson, G. *J. Chem. Soc., Dalton Trans.* **1972**, 1570–1577.
(30) Baumann, J. A.; Salmon, D. J.; Wilson, S. T.; Meyer, T. J.; Hatfield, W. E. *Inorg. Chem.* **1978**, *17*, 3342–3350.
(31) Baranovskii, I. B.; Mazo, G. Ya.; Dikareva, L. M. *Russ. J. Inorg. Chem. (Engl. transl.)* **1971**, *16*, 1388–1389.
(32) Glowiak, T.; Kubiak, M.; Szymanska-Buzar, T. *Acta Crystallogr., Sect. B: Struct. Crystallogr. Cryst. Chem.* **1977**, *B33*, 1732–1737.

0002-7863/87/1509-6341$01.50/0

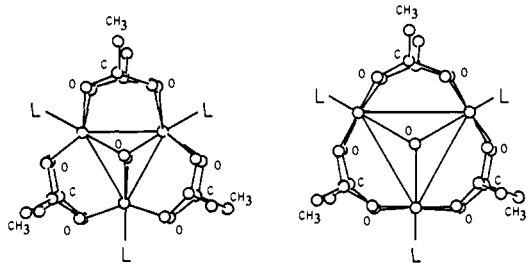

(a) (b)

Figure 1. Structures of the trinuclear complexes discussed in this paper: (a) $[M_3(\mu_3\text{-}O)_2(\mu\text{-}CH_3COO)_6(L)_3]^{2+}$ and (b) $[M_3(\mu_3\text{-}O)(\mu\text{-}CH_3COO)_6(L)_3]^{+}$.

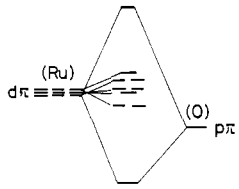

Figure 2. Qualitative molecular orbital scheme for π systems of $[Ru_3(\mu_3\text{-}O)(\mu\text{-}CH_3COO)_6(L)_3]^{+}$.[30]

mixed-metal clusters. Available data of X-ray structural analyses indicate that the metal–metal distances are around 3.3 Å,[7,22,24-27,32] and it is concluded that a direct metal–metal bond is virtually absent. Mixed-metal complexes are known for the Fe–Cr couple.[4,7,9,12,15,33] Magnetic properties of the Fe–Cr mixed-metal clusters are interpreted in terms of the antiferromagnetic coupling of isolated metal ions, and the spectroscopic properties are merely the sum of the isolated metal ion chromophores.[12,34]

The triruthenium mono(μ_3-oxo) clusters are interesting, since they show strong absorption bands in the visible region;[30] i.e., a peak at 692 nm (ϵ 5800 per trimer) and a shoulder at ca. 620 nm are reported for $[Ru_3(\mu_3\text{-}O)(\mu\text{-}CH_3COO)_6(py)_3]^{+}$ (py = pyridine).[30] Corresponding absorption bands are not observed for the mononuclear Ru(III) complexes. These bands are attributed to the intracluster transitions, namely the transitions between the orbitals composed of the metal dπ orbitals and the oxo pπ orbital (Figure 2).[30] It is thus interesting to find how such metal–metal interactions occur in mixed-metal complexes containing ruthenium(III) and other tervalent metal ions.

We have chosen a Ru–Rh couple as a target. The trirhodium(III) complex, which is expected to have similar structural characteristics to the corresponding triruthenium(III), has no strong absorption band in the visible region.[23,31,32] This is explained by the same molecular orbital scheme proposed for the triruthenium(III) complex,[30] since with one additional electron in each rhodium(III) ion the molelcular orbitals are fully occupied and no transitions between these orbitals are possible. The total number of d electrons involved in the mixed-metal clusters should be different from that in the Ru_3 complex (15 electrons) and the Rh_3 complex (18 electrons) (in contrast to our previous example, Mo–W clusters, where the total number of d electrons is fixed to 6[14]). The redox and the ligand-substitution properties of the mixed ruthenium–rhodium clusters are also of considerable interest. Cyclic voltammetric studies revealed that $[Ru_3(\mu_3\text{-}O)(\mu\text{-}CH_3COO)_6(py)_3]^{+}$ shows four distinctive reversible one-electron waves in the region from −2 to +2 V vs SSCE (sodium saturated calomel electrode) in acetonitrile.[29,30] Both one-electron-oxidized and -reduced species have been isolated.[29,30] On the contrary, no extensive electrochemical study has been reported for the trirhodium(III) clusters, and the only report indicated that an irreversible reduction wave was observed at ca. −0.9 to −1.0 V vs SCE, both for the aqua and the pyridine complexes.[23] Substitution properties of monomeric ruthenium(III) and rhodium(III) complexes are appreciably different,[35] although both are regarded as typical substitution-inert centers.

In this study, we were able to prepare only diruthenium–rhodium clusters, $[Ru_2Rh(\mu_3\text{-}O)(\mu\text{-}CH_3COO)_6(L)_3]^{+}$ (L = H_2O or pyridine), but they show various interesting properties, which will be discussed in this paper.

Experimental Section

Preparation of Complexes. (1) Preparation and Separation of Mixed Ruthenium–Rhodium Trinuclear Complexes. The preparation method involves reflux of a mixture of ruthenium(III) trichloride, rhodium(III) trichloride, and sodium acetate in acetic acid–water (or acetic acid–methanol) and subsequent separation of the resulting mixture of the trinuclear complexes into its components by cation-exchange column chromatography or preparative liquid chromatography. The relative amount of the mixed-metal cluster (Ru_2Rh) against two homometal clusters depends significantly on the preparation methods employed.

Preparation 1. A solution of $RhCl_3\cdot 3H_2O$ (1 g) in water (10 cm^3) was mixed with a solution of silver acetate (1 g) in a mixture of water (10 cm^3) and acetic acid (30 cm^3) and with a solution of $RuCl_3\cdot 3H_2O$ (0.5 g) in water (10 cm^3). The resulting mixture was diluted with water (30 cm^3) and acetic acid (40 cm^3) and then refluxed for 3 h. After filtration to remove AgCl, the solution was refluxed for a further 7 h and then treated with a cation-exchange column to obtain a solution of a mixture of the trinuclear monocations. The solution was then evaporated to almost dryness. The separation of the trinuclear complexes was carried out by a preparative liquid chromatography using type LC-09 of Japan Analytical Industry Co. Ltd., with a JAIGEL-ODS (A-343-10) column. The sample solution (ca. 2 cm^3) was injected, and the complexes were eluted at 6 cm^3/min with 0.04 M aqueous $NaClO_4$ solution. Complete resolution was attained after ca. 1 h to obtain pure Ru_2Rh species separated from another main component, Rh_3.

After the mixture (before the separation procedures) was converted directly to the pyridine complexes and the ^{1}H NMR spectrum was measured in CD_2Cl_2, it was found that the ratio of the Rh_3 and the Ru_2Rh by this preparation method is approximately 1:4 and the Ru_3 complex is negligible.

Preparation 2. $RuCl_3\cdot 3H_2O$ (0.2 g) was dissolved in a mixture of methanol (7 cm^3) and acetic acid (7 cm^3), and the solution was refluxed. After 2 h, to the solution was added a solution of $RhCl_3\cdot 3H_2O$ (0.2 g) in a mixture of methanol (5 cm^3) and acetic acid (5 cm^3), and the reflux was continued. Sodium acetate (0.5 g) was added after 2 h, and the reflux was continued for a further 8 h under the slow bubbling of dioxygen. The solution was centrifuged to remove sodium acetate and evaporated to dryness. The residue was dissolved in a large amount of water and passed through a cation-exchange column (Dowex 50W-X2). Elution with 2 M $NaClO_4$ gave a dark blue solution, which contained monocations of the mixed-metal and the homometal trinuclear clusters. The eluate was diluted with a large amount of water and again passed through the cation-exchange column (Dowex 50W-X2; 90 cm in length and 2.9 cm in diameter). On elution with 0.04 M $NaClO_4$ using the two columns of similar size one after another, the components slowly separated. Complete separation was not attained, however, even after more than 3 weeks. Violet eluate of the mixed-metal cluster (Ru_2Rh) was preceded by the yellow eluate of the trirhodium(III) cluster and followed by the blue eluate of the triruthenium(III) cluster. The violet component was obtained in several fractions, absorption spectra of which were carefully measured in order to find purity of the mixed-metal cluster. Spectroscopically pure fractions were used to obtain pure samples of the pyridine complex.

The 400-MHz ^{1}H NMR spectrum revealed that this preparation method gives Ru_3, Ru_2Rh, and Rh_3 clusters in a ratio of approximately 1:4:3.

Preparation 3. $RuCl_3\cdot 3H_2O$ (0.5 g), $RhCl_3\cdot H_2O$ (0.5 g), and sodium acetate (2 g) were dissolved in a mixture of methanol (35 cm^3) and acetic acid (35 cm^3), and the solution was refluxed for 4 h. The solution was then evaporated to dryness. The residue was treated in a manner similar to that in preparation 1. The 400-MHz ^{1}H NMR spectrum shows that this method gives Ru_3, Ru_2Rh and Rh_3 complexes in an approximate 2:6:1 ratio.

(2) (μ_3-Oxo)hexakis(μ-acetato)triaquadiruthenium(III)rhodium(III) Perchlorate, $[Ru^{III}_2Rh^{III}(\mu_3\text{-}O)(\mu\text{-}CH_3COO)_6(H_2O)_3]ClO_4$. By evapora-

(33) A number of mixed-metal clusters of this type are known with two tervalent Fe ions and one divalent ion such as Co, Zn, etc. See for example: (a) Blake, A. B.; Yavari, A.; Kubicki, H. *J. Chem. Soc., Chem. Commun.* **1981**, 796–797. (b) Meesuk, L.; Jayasooriya, U. A.; Cannon, R. D. *J. Am. Chem. Soc.* **1987**, *109*, 2009–2016.

(34) See for example: Straughan, B. P.; Lam, O. M.; Earnshaw, A. *J. Chem. Soc., Dalton Trans.* **1987**, 97–99.

(35) Edwards, J. O.; Monacelli, F.; Ortaggi, G. *Inorg. Chim. Acta* **1974**, *11*, 47–104

Table I. ^1H NMR Chemical Shift Data (in ppm) for $[Ru_2Rh(\mu_3\text{-}O)(\mu\text{-}CH_3COO)_6(L)_3]^+$ (L = H_2O, CD_3OD, or Pyridine) and Corresponding Triruthenium(III) and Trirhodium(III) Complexes[a]

	Ru_2Rh	Rh_3	Ru_3
	L = H_2O[b]		
CH_3 acetate	1.95 (2), 2.32 (1)	2.31	1.11
	L = CD_3OD[c]		
CH_3 acetate	1.99 (2), 2.39 (1)	2.30	1.36
	L = pyridine[d]		
CH_3 acetate	1.96 (6), 2.42 (12)	2.18 (18)	4.80 (18)
C–H pyridine			
ortho	8.60 (4), 8.91 (2)	8.77 (6)	0.27 (6)
meta	7.74 (2), 7.96 (4)	7.66 (6)	5.67 (6)
para	8.11,[e] 8.14[e]	8.05 (3)	6.47 (3)

[a] Relative number of protons in parentheses. [b] Relative to DSS at δ 0 in D_2O (pD ~2 with $DClO_4$). [c] Relative to TMS at δ 0 in CD_3OD. The aqua complexes were dissolved in CD_3OD, and the chemical shifts were measured after the completion of the ligand substitution (see text). [d] Relative to TMS at δ 0 in CD_2Cl_2. [e] Two sets of signals are not well resolved. Total intensity of these two signals is 3.

tion of the eluate of the pure Ru_2Rh component, crystals of the perchlorate salt of the aqua complex (ca. 100 mg by preparation 1) were obtained. Anal. Calcd for $[Ru^{III}_2Rh^{III}(\mu_3\text{-}O)(\mu\text{-}CH_3COO)_6(H_2O)_3]\text{-}ClO_4\cdot 5NaClO_4\cdot 2H_2O$ ($C_{12}H_{28}O_{42}Cl_6Na_5Ru_2Rh$): C, 9.76; H, 1.91; Cl, 14.40. Found: C, 9.90; H, 1.98; Cl, 14.29. IR (cm^{-1}): 3430 br, 1630 sh, 1592 m, 1570 m, 1425 s, 1350 w, 1145 s, 1120 s, 1090 s, 695 w, 635 m, 625 m. The complex is easily soluble in water, methanol, and ethanol.

(3) (μ_3-Oxo)hexakis(μ-acetato)tris(pyridine)diruthenium(III)rhodium(III) Perchlorate, $[Ru^{III}_2Rh^{III}(\mu_3\text{-}O)(\mu\text{-}CH_3COO)_6(py)_3]ClO_4$. A small amount of pyridine (ca. 10% in volume) was added to the eluate of the pure Ru_2Rh component, and the solution was refluxed for ca. 20 min. The dark violet crystals were collected by filtration at room temperature and dried in vacuo over P_2O_5. Yield was ca. 200 mg (preparation 1). Anal. Calcd for $C_{27}H_{33}N_3O_{17}ClRu_2Rh$: C, 32.04; H, 3.29; N, 4.15; Cl 3.50. Found: C, 32.05; H, 3.25; N, 4.10; Cl, 3.79. IR (cm^{-1}): 3430 br, 1600 s, 1565 m, 1485 w, 1450 m, 1425 s, 1350 w, 1120 m, 1100 s, 770 w, 695 m, 635 w, 625 w. The pyridine complex is easily soluble in acetone, acetonitrile, and dichloromethane, slightly soluble in alcohols, and insoluble in water. Addition of NH_4PF_6 (in methanol), $NaCF_3SO_3$ (in water), or $NaB(C_6H_5)_4$ (in water) to the methanolic solution of the perchlorate gave the corresponding salt of the pyridine complex.

(4) Other Complexes. (μ_3-Oxo)hexakis(μ-acetato)tris(aquaruthenium(III)) perchlorate, $[Ru^{III}_3(\mu_3\text{-}O)(\mu\text{-}CH_3COO)_6(H_2O)_3]ClO_4$, and ($\mu_3$-oxo)hexakis($\mu$-acetato)tris(pyridineruthenium(III)) perchlorate, $[Ru^{III}_3(\mu_3\text{-}O)(\mu\text{-}CH_3COO)_6(py)_3]ClO_4$, were preapred by modifying[36] the reported methods.[29,30] (μ_3-Oxo)hexakis(μ-acetato)tris(aquarhodium(III)) perchlorate, $[Rh^{III}_3(\mu_3\text{-}O)(\mu\text{-}CH_3COO)_6(H_2O)_3]ClO_4$, and ($\mu_3$-oxo)hexakis($\mu$-acetato)tris(pyridinerhodium(III)) perchlorate, $[Rh^{III}_3(\mu_3\text{-}O)(\mu\text{-}CH_3COO)_6(py)_3]ClO_4$, were prepared by the method[37] based on that described by Baranovskii et al.[31]

Other Materials. Acetonitrile was distilled over P_2O_5 and CaH_2. All other reagents were used as received.

(36) $RuCl_3\cdot 3H_2O$ (1 g) and sodium acetate (2 g) were dissolved in a mixture of methanol (or ethanol) (25 cm^3) and acetic acid (25 cm^3). The solution was refluxed for ca. 6 h and was centrifuged at room temperature to remove sodium acetate. The resulting supernatant liquid was filtered and then evaporated to dryness. The residue was dissolved in 100 cm^3 of methanol, and the solution was again evaporated. The residue was then dissolved in water and treated with a cation-exchange column (Dowex 50W-X2). The cationic species was eluted with 2 M of $NaClO_4$, and the eluate was evaporated to obtain the crystals of the perchlorate salt of the aqua complex. To obtain the pyridine complex, pyridine was added to the above eluate (10% in volume of the eluate), and the solution was refluxed for 20 min. The crystals of the perchlorate salt were collected by filtration, washed with a large amount of water until the smell of pyridine disappeared, and dried over P_2O_5 in vacuo.

(37) An aqueous solution (30 cm^3) of $RhCl_3\cdot 3H_2O$ (1 g) was mixed with a suspension of silver acetate (1 g) in acetic acid (30 cm^3), and the mixture was refluxed for ca. 6 h. Silver chloride was removed by filtration, and the filtrate was evaporated to dryness. The residue was then dissolved in water and treated with a cation-exchange column (Dowex 50W-X2). The eluate with 2 M of aqueous $NaClO_4$ solution was evaporated to give yellow crystals of the perchlorate salt of the aqua complex. To the eluate was added a small amount of pyridine. The solution was then refluxed for 20 min. The precipitate was collected by filtration, washed with water, and dried in vacuo over P_2O_5.

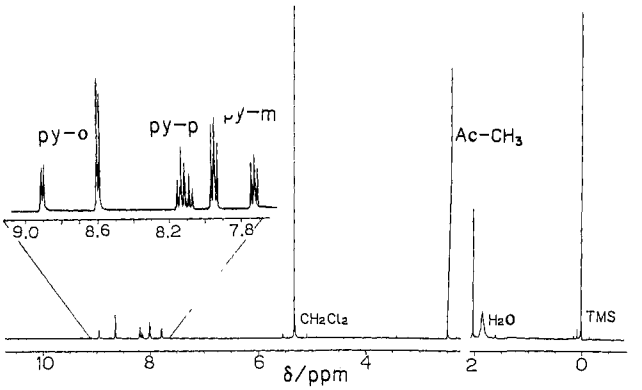

Figure 3. 400-MHz ^1H NMR spectrum of $[Ru_2Rh(\mu_3\text{-}O)(\mu\text{-}CH_3COO)_6(py)_3]ClO_4$ in CD_2Cl_2 at 21 °C.

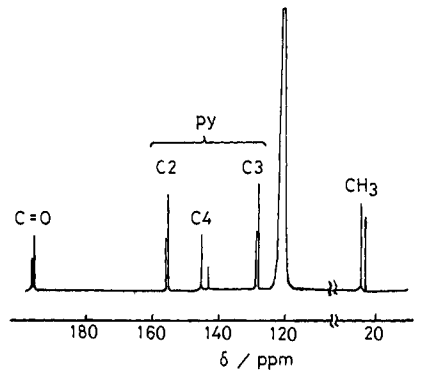

Figure 4. ^{13}C NMR spectrum of $[Ru_2Rh(\mu_3\text{-}O)(\mu\text{-}CH_3COO)_6(py)_3]\text{-}ClO_4$ in CD_3CN (δ 0 for TMS).

Table II. ^{13}C NMR Chemical Shift Data (in ppm) for $[M_3(\mu_3\text{-}O)(\mu\text{-}CH_3COO)_6(py)_3]^+$ in CD_3CN Relative to TMS at δ 0

	M_3		
	Ru_2Rh[a]	Rh_3	Ru_3
CH_3 (acetate)	22.3 (Ru—Ru), 23.7 (Ru—Rh)	25.3	114.8
C=O (acetate)	194.5 (Ru—Ru), 193.7 (Ru—Rh)	188.4	199.0
C-2 (pyridine)	153.4 (Ru), 153.8 (Rh)	152.8	−6.2
C-3 (pyridine)	126.0 (Ru), 126.8 (Rh)	126.4	138.3
C-4 (pyridine)	143.1 (Ru), 140.9 (Rh)	140.4	126.8

[a] Assignments of these peaks are made by considering relative intensities.

Measurements. Ultraviolet and visible absorption spectra were measured with use of Hitachi 330 and 340 spectrophotometers. Infrared absorption spectra were recorded on a Jasco IR-810 spectrophotometer as KBr pellets at room temperature. X-ray photoelectron spectra were obtained by a VG-ESCA LAB Mark II using Mg Kα exciting radiation at ambient temperature at pressure less than 10^{-9} Torr. The energy scale was calibrated by emission from the C 1s (methyl carbon) line at 284.6 eV. Samples were prepared as thin films on Ni or Al metal by evaporating acetonitrile solutions. Electrochemical measurements were carried out by using a YANACO P-1100 polarographic analyzer with a glassy-carbon working electrode at 24 ± 2 °C. Potential was recorded vs a Ag/Ag^+ electrode. The 400-MHz ^1H NMR spectra were measured on a JEOL JNM-GX-400 FT-NMR spectrometer. ^{13}C NMR spectra were obtained by a Varian XL-200 FT-NMR spectrometer. X-ray powder diffraction patterns were obtained by Rigaku Geigerflux.

Results

1. ^1H and ^{13}C NMR Spectra. ^1H and ^{13}C NMR spectra of $[Ru_2Rh(\mu_3\text{-}O)(\mu\text{-}CH_3COO)_6(py)_3]^+$ are shown in Figures 3 and 4, respectively. All the chemical shift data including those of the homometal trimers are summarized in Tables I and II. The ^1H NMR data for the two homometal clusters are in reasonable agreement with the previous reports.[23,30] The ^{13}C NMR data are reported for the first time for these clusters. As noted previously for the ^1H NMR,[30] paramagnetic shifts of both ^1H and ^{13}C NMR are small for paramagnetic triruthenium(III) complexes. The pyridine proton signals can be unambiguously assigned to ortho,

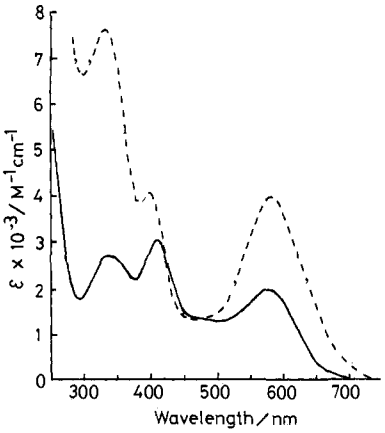

Figure 5. Electronic absorption spectra of $[Ru_2Rh(\mu_3\text{-}O)(\mu\text{-}CH_3COO)_6(H_2O)_3]ClO_4$ (—) in water at pH 1.85 ($HClO_4$) and of $[Ru_2Rh(\mu_3\text{-}O)(\mu\text{-}CH_3COO)_6(py)_3]ClO_4$ (---) in methanol at room temperature.

Table III. Numerical Data of Ultraviolet–Visible Absorption Spectra of $[Ru_2Rh(\mu_3\text{-}O)(\mu\text{-}CH_3COO)_6(L)_3]^+$

L	solvent	λ, nm (ε, M^{-1} cm^{-1})
H_2O	water	576 (2000), 480 sh, 408 (3120), 336 (2730)
pyridine	methanol	586 (3980), 403 (4140), 332 (7660)
CH_3OH	methanol	581 (2200), 480 sh, 416 (3480), 335 (3120)

meta, and para protons (as in Table I) from the splitting patterns and relative integrated intensities. The ^{13}C NMR signals of the coordinated pyridines can be assigned by comparison to those of free pyridines (C-2, 150.2; C-3, 123.9; and C-4, 135.9 ppm) and by relative intensity ratio.

The methyl proton signal of the coordinated acetate appears as a sharp singlet for the aqua and the pyridine complexes of Ru_3 and Rh_3, but those for Ru_2Rh split into two peaks with a 1:2 integrated intensity ratio. For the pyridine complex of Ru_2Rh, the ortho and meta hydrogen signals of the coordinated pyridines split, respectively, into two groups with a 1:2 integrated intensity ratio. The para hydrogen signals are seen, however, as one group, since the splitting is small. Signals of the ortho protons of the pyridine coordinated to Rh appear at lower field than those coordinated to Ru, while signals of the meta protons appear at higher field for the pyridine coordinated to Rh. In the case of the ^{13}C NMR, signals of the pyridines coordinated to Ru appear at higher field for the C-2 and the C-3 carbons and at lower field for the C-4 carbons. The signals of the pyridine at the rhodium ion in the mixed-metal cluster always appear at slightly lower field than those in the trirhodium(III) cluster.

The change in the unindentate ligands (H_2O, pyridine, or CD_3OD) gave small but distinctive shifts of the acetate methyl proton signals for the two clusters, Rh_3 and Ru_2Rh. The methyl signals of the aqua complexes show very small differences between values obtained in D_2O (pD ~2 with $DClO_4$) and those obtained in CD_3OD (measured immediately after dissolution, before the ligand substitution takes place) for the Rh_3 and Ru_2Rh complexes.

2. Electronic and Infrared Absorption Spectra. Absorption spectra of the new mixed-metal clusters are shown in Figure 5. Numerical data are summarized in Table III. Both the aqua and the pyridine complexes of the Ru_2Rh show intense absorption bands in the visible region. Such strong absorption bands are observed also for the Ru_3 clusters, but not for the Rh_3 clusters. The spectra of the aqua complexes in methanol are clearly different from those in aqueous solution. The former should correspond to the species, $[M_3(\mu_3\text{-}O)(\mu\text{-}CH_3COO)_6(CH_3OH)_3]^+$ (vide infra).

The strong absorption band of lowest energy appears at a shorter wavelength for the Ru_2Rh clusters than for the Ru_3 clusters. An additional band in the visible region is observed at ca. 410 nm for the Ru_2Rh clusters, and there is clearly a shoulder at around 490 nm. These features in the visible region are commonly seen regardless of the unidentate ligands and should be ascribed to the transitions within the mixed-metal Ru_2RhO core. One-electron-reduced species of the triruthenium(III) complex, $Ru_3(\mu_3\text{-}O)(\mu\text{-}CH_3COO)_6(py)_3$, is isoelectronic with the present mixed-metal clusters. This neutral triruthenium complex has strong bands at the lower energy side (>800 nm) as well as the bands in the region 400–500 nm.[30] The Ru_2Rh cluster does not have any strong absorption bands toward the near-infrared region.

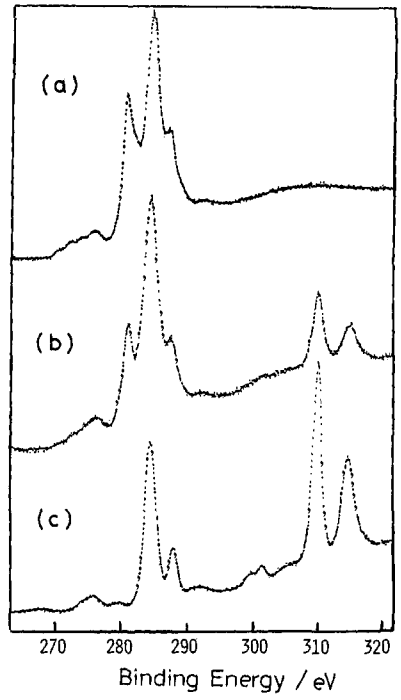

Figure 6. X-ray photoelectron spectra of the three complexes, $[M_3(\mu_3\text{-}O)(\mu\text{-}CH_3COO)_6(py)_3]ClO_4$, at the Ru 3d and Rh 3d regions (binding energies are calibrated for the C 1s peak at 284.6 eV): (a) $M_3 = Ru_3$, (b) $M_3 = Ru_2Rh$, and (c) $M_3 = Rh_3$.

The $\nu_{asym}(C{=}O)$ region of the IR spectra shows characteristic differences among the complexes of three different trinuclear cores. The aqua complexes of the Ru_3 and the Rh_3 show one sharp band at 1560 and 1600 cm^{-1}, respectively, while that of the Ru_2Rh has two peaks at 1592 and 1570 cm^{-1}. Similar features are also observed for the pyridine complexes.

3. X-ray Photoelectron Spectra. Figure 6 shows the Ru 3d and Rh 3d region of the XPS spectra of the perchlorate salts of the Ru_3–, Ru_2Rh–, and Rh_3–pyridine complexes. Comparison of the XPS peak intensities of the Ru_2Rh complex with those of the Rh_3 and Ru_3 complexes confirmed that the ratio of Ru to Rh in the mixed-metal cluster is 2:1.

The Rh $3d_{3/2}$ and $3d_{5/2}$ binding energies were found to be 314.3 and 309.6 eV, respectively, for both Rh_3 and Ru_2Rh complexes. The Ru $3d_{5/2}$ peak for the Ru_3 complex appears at 281.0 eV, while the Ru $3d_{3/2}$ peak is masked by the strong C 1s peak at 284.6 eV, which was used as a standard. An identical value (281.0 eV) was obtained for the hexafluorophosphate salt, for which the reported value is 280.6 eV (calibrated for the C 1s peak position as 284.4 eV).[30] The mixed-metal complex shows the Ru $3d_{5/2}$ peak at 281.3 eV. The difference in the Ru $3d_{5/2}$ binding energies between the Ru_3 and Ru_2Rh complexes is small but is clearly out of the uncertainty range.

For the mixed molybdenum–tungsten clusters, the differences in binding energies of Mo 3d, W 4d, and W 4f electrons between the mixed-metal clusters, Mo_2W and MoW_2, and the homometal clusters, Mo_3 and W_3, are significantly larger (0.5–1 eV).[17] The Mo 3d binding energy decreases, and the W 4d and 4f binding energies increase with an increase in the number of Mo atoms in the trinuclear core. The results were explained by the negative charge shift from W to Mo along the Mo–W bond.[17] The XPS data indicate that such a charge shift does not occur in the present Ru_2Rh complex, which is consistent with the much weaker metal–metal direct interaction of these types of trinuclear complexes.

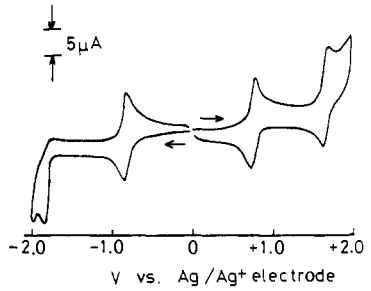

Figure 7. Cyclic voltammogram of $[Ru_2Rh(\mu_3\text{-}O)(\mu\text{-}CH_3COO)_6(py)_3]ClO_4$ at room temperature in 0.1 M $(n\text{-}Bu_4N)ClO_4$ in CH_3CN (V vs Ag/Ag^+ electrode) at a scan rate of 50 mV/s.

Table IV. Electrochemical Data for the Clusters $[M_3(\mu_3\text{-}O)(\mu\text{-}CH_3COO)_6(py)_3]^m$ (m = +3 to −1) in 0.1 M $[(n\text{-}C_4H_9)_4N]ClO_4$ in CH_3CN at 24 ± 2 °C

	$E_{1/2}$ ($E_{ap} - E_{cp}$, mV)[a]			
M_3	+3/+2[b]	+2/+1[b]	+1/0[b]	0/−1[b]
Ru_3	+1.67 (70)	+0.74 (60)	−0.32 (60)	−1.59 (60)
Ru_2Rh	+1.68 (70)	+0.79 (60)	−0.77 (60)	
Rh_3		+0.99 (90)		

[a] $E_{1/2}$ in volts vs the Ag/Ag^+ electrode. [b] Redox processes are expressed by overall charges of the complexes.

4. Electrochemical Properties. The redox properties of Ru_2Rh clusters were studied with the pyridine complex by means of cyclic voltammetry. A cyclic voltammogram is shown in Figure 7. The $E_{1/2}$ values are summarized in Table IV together with the corresponding data of the homonuclear complexes. The data for the Ru_3 complex are in good agreement with those reported in the literature.[29,30] The $E_{1/2}$ value of the Rh_3 complex is reported for the first time.

The Ru_2Rh cluster has three redox waves in the region from −2 and +2 V vs Ag/Ag^+ electrode. All of these waves are essentially reversible. These redox processes are assigned to one-electron processes by comparing peak heights with those of the Ru_3 cluster. Two oxidation processes are observed at potentials nearly identical with those of the Ru_3 complex. As to the reduction process, the mixed-metal cluster shows only one wave in contrast to the two waves observed for the Ru_3 cluster. In the case of the Rh_3 cluster, only one oxidation wave is observed.

5. Ligand-Substitution Properties. ^1H NMR spectra of the aqua complex of Ru_2Rh in CD_3OD provide information on the successive substitution of methanol for the aqua ligands (Figure 8). Each of the two methyl singlets of the parent aqua complex splits into three and four with time, while the relative intensity ratio of the two groups of signals remains unchanged. The final spectrum with two methyl singlets in a 1:2 intensity ratio should correspond to $[Ru_2Rh(\mu_3\text{-}O)(\mu\text{-}CH_3COO)_6(CD_3OD)_3]^+$.

For the methyl signals of the acetate bridging two ruthenium ions, signals at 1.92, 1.96, and 2.00 ppm are assigned to the acetate bridging two Ru–H_2O, Ru–H_2O and Ru–CD_3OD, and two Ru–CD_3OD, respectively. For the methyl signals of the acetate bridging Ru and Rh, signals at 2.37 and 2.39 ppm are assigned to the acetate bridging Ru–H_2O and Rh–H_2O, and Ru–CD_3OD and Rh–CD_3OD, respectively. The signals at 2.36 and 2.40 ppm should be assigned to the acetate bridging Ru–H_2O and Rh–CD_3OD, and Ru–CD_3OD and Rh–H_2O. Since these two peaks behave in an almost identical way, the rates of substitution at Ru and Rh should be very similar to each other. It seems that the unidentate ligand does not affect the chemical shift of the acetate methyl groups at the opposite side, since additional splitting was not observed. Figure 9 shows the reaction scheme of the substitution reactions. Reactions proceed via multisteps, and the kinetic analysis for obtaining all the rate constants is very complicated. Nevertheless, the initial decrease in the intensities of the two original peaks enables us to obtain the rate constants of initial substitution processes, k_1 and k_4. The plot of logarithmic relative intensity (%) against time gave a good straight line for the signal of the acetate (Rh(H_2O)–Ru(H_2O)). The slope gives

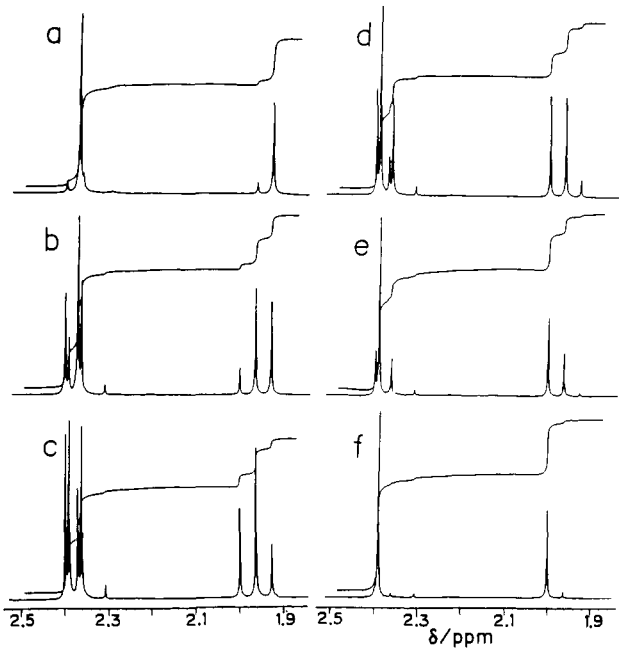

Figure 8. Time dependence of the ^1H NMR spectrum of $[Ru_2Rh(\mu_3\text{-}O)(\mu\text{-}CH_3COO)_6(H_2O)_3]ClO_4$ in CD_3OD at 21 °C: (a) 13 min, (b) 2 h, (c) 4 h, (d) 6 h, (e) 10 h, and (f) 25 h after the dissolution.

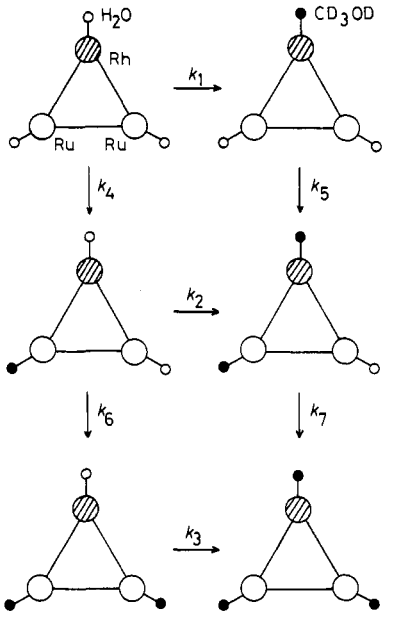

Figure 9. Diagram for the successive substitution of CD_3OD for water in $[Ru_2Rh(\mu_3\text{-}O)(\mu\text{-}CH_3COO)_6(H_2O)_3]^+$ in CD_3OD.

a rate constant, 1.80×10^{-4} s^{-1}, that should correspond to ($k_1 + k_4/2$).[38] A similar plot for the methyl signal of the acetate (Ru(H_2O)–Ru(H_2O)) is also a straight line. From the slope of the straight line, the first-order rate constant, 1.20×10^{-4} s^{-1} at 21 °C, was obtained, which should correspond to k_4,[39] the replacement of the first water ligand of the two aqua–ruthenium complexes. For one particular ruthenium ion, the rate constant should be 6.0×10^{-5} s^{-1}. The rate constant for the substitution at rhodium center, k_1, was estimated to be 1.20×10^{-4} s^{-1}. The substitution rate constants for the Ru and Rh centers are very similar to each other, and it is concluded that there is no significant site selectivity at least for the present reaction.

(38) The decrease in intensity of this peak should involve the contribution of k_6, which is, however, negligible at the initial part of the decrease.
(39) The decrease in intensity of this peak should involve the contribution of k_5, which is, however, negligible at the initial part of the decrease.

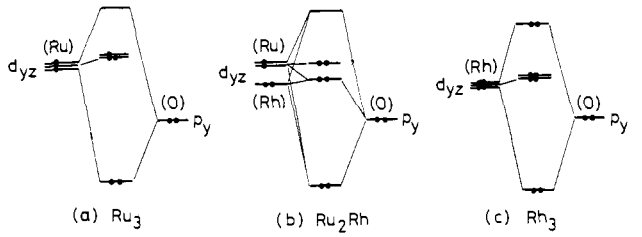

Figure 10. Simplified qualitative molecular orbital scheme for the π systems involving one $d\pi$ orbital of each metal ion and one $p\pi$ orbital of the central oxygen for the clusters, $[M_3(\mu_3\text{-}O)(\mu\text{-}CH_3COO)_6(L)_3]^+$ (M_3 = Ru_3, Ru_2Rh, and Rh_3) (for Ru_3, the orbital with the unpaired electron can be composed of the other two $d\pi$ orbitals of the metal ions[30]).

Discussion

1. Characterization of Mixed-Metal Clusters. X-ray powder patterns of the pyridine complexes of Ru_3, Ru_2Rh, and Rh_3 are very similar to one another. This fact, as well as the behavior of the column chromatography, indicates that the new complex has very similar structural characteristics to the known Ru_3 and Rh_3 complexes.

The most conclusive evidence for the mixed-metal trinuclear cluster core comes from the ^1H and ^{13}C NMR spectra. All the peaks of acetate ions clearly split into two with a 1:2 integrated intensity ratio. Split of the pyridine signals also unambiguously supports the mixed-metal structure.

The ratio of the two kinds of metal ions in the cluster unit was determined by the XPS spectra. Also, the observation of the ^1H and ^{13}C NMR signals in essentially "diamagnetic" region is consistent with the Ru_2Rh structure rather than the $RuRh_2$ one, the latter being expected to have at least one unpaired electron.

It should be noted that no positive evidence for the existence of the $RuRh_2$ cluster was found under any experimental conditions employed. Even if the excess $RhCl_3\cdot 3H_2O$ to $RuCl_3\cdot 3H_2O$ was used as starting material, a large amount of the Rh_3 complex together with only the Ru_2Rh complex was produced. There seems to be no particular reason why the $RuRh_2$ cluster is unstable or cannot exist. The fact that the $RuRh_2$ cluster is not found may be related to the mechanism of the formation of the trinuclear clusters. The synthetic routes employed in this work may be inappropriate to produce the $RuRh_2$ cluster.

2. Electronic Structure of New Mixed Ruthenium–Rhodium Clusters. The Ru_3 complexes show intense absorption peaks in the visible region.[29,30] Meyer and co-workers have explained these transitions in terms of the molecular orbital scheme in Figure 2 and assigned these transitions from the lower occupied orbitals to the highest unoccupied one.[30] Although X-ray structural analysis has been carried out only for the Rh_3 complex (Rh–Rh distance, 3.3 Å),[32,40] it is very unlikely that the structural characteristics are significantly different between the Ru_3 and Rh_3 complexes, since all the known metal–metal distances of other trinuclear clusters of this type, such as Cr_3, Fe_3, and others, are around 3.3 Å.[22,24-27] Under the assumption that the structures of all three clusters, Ru_3, Ru_2Rh, and Rh_3, are not significantly different, similar molecular orbital schemes may be considered for the Ru_2Rh and Rh_3 complexes. If we take the z axis of one particular metal atom in the trinuclear cluster as the direction of oxygen atom and the y axis as the perpendicular direction to the M_3O plane, only the d_{yz} orbital among the three $d\pi$ orbitals has significant interaction with the oxygen $p\pi$ (p_y) orbital. Two other $d\pi$ orbitals essentially remain as nonbonding molecular orbitals with regard to the interaction with the central oxygen (Figure 2). To simplify the scheme, we only consider the interaction of the metal d_{yz} orbitals and the oxygen $p\pi$ orbital. Figure 10 shows such simplified molecular orbital schemes for the three clusters. Here, the lowest orbital is bonding and the highest one is antibonding in nature. The remaining two orbitals are essentially nonbonding. The NMR behavior of the Ru_2Rh cluster is consistent with this scheme.

The absence of any strong absorption band in the visible region of the Rh_3 complexes is reasonable, since all the orbitals are totally full with 18 electrons from the three d^6 metal ions. In the mixed-metal clusters, the highest orbital is now vacant, and visible absorption bands should thus be assigned to the transitions to this vacant orbital from the lower occupied orbitals.

The blue shift of the lowest energy band in the Ru_2Rh cluster seems to indicate that the nonbonding orbitals are more stabilized than the Ru_3 by the participation of Rh^{III} with more stabilized $d\pi$ orbitals. This is compared with the isoelectronic neutral triruthenium species (Ru_3 has 16 electrons with a formal (III, III, II) oxidation state), which shows red shift of the corresponding bands, where the destabilization of the nonbonding orbitals by increasing electron population appears to be more important.[30]

The redox processes observed for the Ru_3 have unambiguously assigned to occur at cluster core Ru_3O and not at ligand pyridines.[30] In the Ru_2Rh cluster, all the processes should also occur at the cluster core, Ru_2RhO. The two successive one-electron-oxidation processes in the mixed-metal cluster show very similar potentials to those of the Ru_3 cluster. Such similarity may be related to the expectation that in both cases electrons may be removed from the nonbonding orbitals with essentially ruthenium character. The reduction process of the Ru_2Rh cluster should involve the addition of one electron to the antibonding orbital and thus occurs with more difficulty than the first reduction process of the Ru_3 cluster. The process occurs more easily, however, than the second reduction process of the Ru_3 cluster (to add a second electron to the antibonding orbital), probably by the participation of Rh^{III} with more stabilized orbitals. In summary, the rhodium ion in the Ru_2Rh cluster does not participate significantly in the observed redox processes.

3. Reactivity of Mixed-Metal Clusters. The mixed-metal cluster does not show site selectivity in the substitution reactions of unidentate ligands. Available data on the ligand-substitution reactions of the mononuclear complexes of Ru^{III} and Rh^{III} show that Ru^{III} is somewhat more labile than Rh^{III} although quantitative comparison is difficult since the reaction systems and experimental conditions are not always comparable.[35] Kido and Saito have pointed out that there is a good linear correlation with slope of unity between log k_{H_2O} and log k_{acac} for a series of tervalent metal ions, where k_{H_2O} and k_{acac} are the water-exchange rate constant for $[M^{III}(H_2O)_6]^{3+}$ in water and the acetylacetonate-exchange rate constant for $[M^{III}(acac)_3]$ in neat acetylacetone, respectively.[41] The acetylacetonate-exchange rates are slower for the rhodium(III) than for the ruthenium(III) by about 2 orders of magnitude.[42] This difference may be taken as a good measure of the difference in substitution labilities of the two tervalent metal ions.[41]

The absence of the site selectivity in the Ru_2Rh cluster indicates the disappearance of the original difference in labilities of the two metal centers. Also, the rate constants obtained here are several orders of magnitude larger than the ligand-substitution rate constants of mononuclear species.[35] Our preliminary results on the substitution of methanol for the aqua ligands of $[Ru_3(\mu_3\text{-}O)(\mu\text{-}CH_3COO)_6(H_2O)_3]^+$ and $[Rh_3(\mu_3\text{-}O)(\mu\text{-}CH_3COO)_6(H_2O)_3]^+$ in methanol at 21 °C show first-order rate constants, 1.7×10^{-3} and 3×10^{-3} s^{-1}, respectively.[43] The difference in the two rate constants is small. Thus the disappearance of the difference in the labilities between the two metal ions is caused by the trinuclear complex formation rather than by the mixed-metal complex formation. Another interesting point is that the rate constants for the Ru_2Rh complex are smaller by nearly 1 order of magnitude than those for the Ru_3 and Rh_3 complexes. This fact suggests that the metal–metal interactions also play some role in substitution lability. With limited available data on lig-

(40) X-ray structural analysis has been carried out for one-electron-reduced species, $[Ru_3(\mu_3\text{-}O)(\mu\text{-}CH_3COO)_6(P(C_6H_5)_3)_3]$, in which the Ru–Ru distance is 3.329 Å. Cotton, F. A.; Norman, J. G., Jr. *Inorg. Chim. Acta* **1972**, *6*, 411–419.

(41) Kido, H.; Saito, K., to be submitted for publication.

(42) Kido, H. *Bull. Chem. Soc. Jpn.* **1980**, *53*, 82–87.

(43) Sasaki, Y.; Nagasawa, A.; Tokiwa, A.; Ito, T. Presented at the XXV International Conference on Coordination Chemistry, Nanjing, People's Republic of China, July 1987; Abstract C2-415.

and-substitution reactions of the trinuclear complexes, it is not possible to further discuss these interesting findings.

Acknowledgment. We thank the Instrument Center, the Institute for Molecular Science, for assistance in obtaining the XPS spectra. We also thank Japan Analytical Industry Co. Ltd., for the preparative liquid chromatography, and Professor Y. Shono and Dr. K. Kusaba (Research Institute for Iron, Steel, and Other Metals, Tohoku University), for the measurements of the X-ray powder diffraction patterns.

Photoactivation of Metal Oxide Surfaces: Photocatalyzed Oxidation of Alcohols by Heteropolytungstates

Marye Anne Fox,* Raul Cardona, and Elizabeth Gaillard

Contribution from the Department of Chemistry, The University of Texas at Austin, Austin, Texas 78712. *Received January 9, 1987. Revised Manuscript Received May 20, 1987*

Abstract: Photoinduced oxidation of primary, secondary, and tertiary alcohols by several tungstates of varying structural complexity ($WO_2(OR)_2$, $PW_{12}O_{40}^{3-}$, or $(WO_3)_n$) requires strong alcohol precomplexation before photoactivation and occurs via a rapid two-electron transfer, in contrast to previous mechanistic suggestion. The relative efficiencies for alcohol oxidation induced by excitation of a series of heteropolytungstates of increasing molecular complexity are reported. Mechanistic features of the photocatalytic oxidation are described, and a comparison is drawn between thermal and photochemical activation of the heteropolytungstates.

A fundamental problem in catalysis is to identify and characterize reactions that can be induced by heat or by light. Contrasting chemical behavior observed upon thermal or photochemical activation can provide information valuable in understanding surface–solute interactions and the effect of the catalyst on relative activation energies of competing pathways. Recent reports of photocatalytic oxidation of organic substrates on heteropolyoxoanions excited by ultraviolet wavelengths,[1-11] together with previous reports of thermal oxidative catalysis on these same substrates,[12-14] make this family of compounds an attractive target for such mechanistic investigations. Furthermore, our interest in the nature of fundamental interactions of organic molecules on the surfaces of irradiated metal oxide semiconductors[15,16] has led us to investigate the photocatalytic reactions of these species as soluble analogues of semiconductor metal oxide suspensions.

Transition-metal oxides represent species that span the range from discrete molecules to extended semiconductor structures. As a subset of this class, the polyoxoanions possess structures that are well characterized at the molecular level[13,14] and acidity and redox properties that can be systematically controlled. The heteropolyoxometalates consist of a single atom (P, Si, Co, etc.) surrounded by metal oxide units, constituting arrays that may contain up to 200 or more atoms. For the usual oxidation levels

Table I. Heteropolyoxoanions Evaluated as Photocatalysts

cation	central atom[a]	size
$H_3PW_{12}O_{40}\cdot 30H_2O$	$Na_3PW_{12}O_{40}\cdot 10H_2O$	$WO_2(OR)_2$
$Na_3PW_{12}O_{40}\cdot 10H_2O$	$Na_6H_2W_{12}O_{40}\cdot 22H_2O$	$Na_3PW_{12}O_{40}\cdot 10H_2O$
$(NH_4)_3PW_{12}O_{40}\cdot 10H_2O$	$K_4SiW_{12}O_4\cdot 8H_2O$	$(NH_4)_6P_2W_{18}O_{62}\cdot 30H_2O$
$(Pr_4N)_3PW_{12}O_{40}\cdot 10H_2O$	$H_5(FeW_{12}O_{40})\cdot 10H_2O$	$(NH_4)_{14}NaP_5W_{30}O_{110}\cdot 31H_2O$
	$K_5HCoW_{12}O_{40}\cdot 15H_2O$	$(Bu_4N)_5H_4P_2W_{15}V_3O_{62}$[b]
		$(Bu_4N)_4H_3SiW_9V_3O_{40}$[b]
		$(WO_3)_n$[c]
		$(WO_3)_n$/Pt

[a] The band gap of WO_3 is close to 2.7 eV, which corresponds approximately to 459 nm.[46] [b] These samples were a gift from R. G. Finke, University of Oregon. [c] Reference 46.

Table II. Solubility of Salts of **1**

	salt		
solvent	Na^+ ($\cdot H_2O$) rt[a]/Δ	NH_4^+ ($\cdot H_2O$) rt/Δ	Pr_4N^+ ($\cdot H_2O$) rt
water	PS/S[b]	I/S	I
ether	I/I	I/I	I
acetone	PS/PS	I/I	I
1,4-dioxane	I/I	I/I	I
acetonitrile	PS/PS	I/I	S
CCl_4	I/–	I/–	I
$CHCl_3$	I/–		
CH_2Cl_2	I/I	PS/PS	I
acetic anhydride	I/I	I/I	
DMF	PS/PS	PS/S	S
DMSO	S (yellow)/S	I/S (after a day)	S (yellow)
pyridine	C/PS, C	C/I	
methanol	S/S	I/I	I
ethanol	PS/PS	I/I	

[a] rt = room temperature. [b] S = soluble; PS = partially soluble; I = insoluble; C = cloudy.

(1) Papaconstantinou, E. *Chem. Commun.* **1982**, 12.
(2) Papaconstantinou, E.; Dimotikali, D.; Politou, A. *Inorg. Chim. Acta* **1980**, *43*, 155.
(3) Darwent, J. R. *Chem. Commun.* **1982**, 798.
(4) Papaconstantinou, E.; Dimotikali, D. *Inorg. Chim. Acta* **1984**, *87*, 177.
(5) Ward, M. D.; Brazdil, J. F.; Grasselli, R. K. *J. Phys. Chem.* **1984**, *88*, 4210.
(6) Yamase, T.; Kurozumi, T. *J. Chem. Soc., Dalton Trans.* **1983**, 2205.
(7) Yamase, T. *Inorg. Chim. Acta* **1981**, *54*, L207.
(8) Yamase, T. *J. Synth. Org. Chem. Jpn.* **1985**, *43*, 249.
(9) Renneke, R. F.; Hill, C. L. *J. Am. Chem. Soc.* **1986**, *108*, 3528.
(10) Argitis, P.; Papaconstantinou, E. *J. Photochem.* **1985**, *30*, 445.
(11) Hill, C. L.; Bouchard, D. A. *J. Am. Chem. Soc.* **1985**, *107*, 5148.
(12) Kozhevnikov, I. V.; Matveev, K. I. *Russ. Chem. Rev. (Engl. Transl.)* **1982**, *51*, 1075.
(13) Pope, M. T. *Heteropoly and Isopoly Oxometalates*; Springer-Verlag: New York, 1983.
(14) Day, V. W.; Klemperer, W. G. *Science (Washington, D.C.)* **1985**, *228*, 533.
(15) Fox, M. A. *Acc. Chem. Res.* **1983**, *16*, 314.
(16) Fox, M. A. *NATO Adv. Sci. Inst. Ser.* **1986**, *174*, 363.

0002-7863/87/1509-6347$01.50/0